Published in final edited form as:
Small. 2009 November ; 5(22): 2618–2624. doi:10.1002/smll.200900937.

Sniffing the Unique "Odor Print" of Non-Small-Cell Lung Cancer with Gold Nanoparticles

Orna Barash,
Department of Chemical Engineering and Russell Berrie Nanotechnology Institute Technion–Israel Institute of Technology Haifa 32000 (Israel)

Nir Peled,
University of Colorado Cancer Center Division of Medical Oncology Aurora, CO 80045 (USA)

Fred R. Hirsch, and
University of Colorado Cancer Center Division of Medical Oncology Aurora, CO 80045 (USA)

Hossam Haick
Department of Chemical Engineering and Russell Berrie Nanotechnology Institute Technion–Israel Institute of Technology Haifa 32000 (Israel)

Hossam Haick: hhossam@technion.ac.il

Abstract

A highly sensitive and fast-response array of sensors based on gold nanoparticles, in combination with pattern recognition methods, can distinguish between the odor prints of non-small-cell lung cancer and negative controls with 100% accuracy, with no need for preconcentration techniques. Additionally, preliminary results indicate that the same array of sensors might serve as a better tool for understanding the biochemical source of volatile organic compounds that might occur in cancer cells and appear in the exhaled breath, as compared to traditional spectrometry techniques. The reported results provide a launching pad to initiate a bedside tool that might be able to screen for early stages of lung cancer and allow higher cure rates. In addition, such a tool might be used for the immediate diagnosis of fresh (frozen) tissues of lung cancer in operating rooms, where a dichotomic diagnosis is crucial to guide surgeons.

Keywords

breath analysis; lung cancer; nanoparticles; sensors; volatile organic compounds

1. Introduction

Recent statistics have estimated that in Europe in 2004, nearly 2.9 million new cases of cancer were diagnosed and the disease caused over 1.7 million deaths, with lung cancer as the most common form of cancer diagnosed and of cancer death in both men and women.[1,2] The statistics also show that the current five-year ultimate survival rate for lung cancer patients is 15%, but the expected survival rate is >70% if the cancer is discovered when still localized.[3] Unfortunately, only 16% of lung cancer is discovered when it is still in the localized stage and the disease is curable.[2,3] The statistics warn that this figure will

Correspondence to: Hossam Haick, hhossam@technion.ac.il.

continue to rise and that the need exists to consider priorities for cancer control, especially techniques having the maximum effect.

Efforts to identify early detection methods for lung cancer are now at an exciting stage.[3] Serious efforts are being made to assess the role of computed tomography (CT) imaging as a screening technology,[4,5] although still without proven efficiency. Moreover, even after definitive therapy without any evidence of disease, early local recurrence might be detected by a routine bronchoscopy for non-small-cell lung cancer (NSCLC)[6] in 4% of patients treated surgically. Currently, the diagnostic steps for lung cancer include an invasive procedure that yields a tissue specimen, such as cytology and/or histology. By having a tissue specimen, one can specify and tailor therapy according to the histology type, mutation analysis, specific staining (such as for epidermal growth factor receptor, EGFR), and other specifications. However, such procedures are invasive, expensive, and might delay therapy. Moreover, they are not free from complications; for example, up to 2.5% complications and 0.5% mortality occur for mediastinoscopy[7] and 0.3% major complications for transbronchial needle aspiration bronchoscopy.[8] In addition, the sensitivity of such tests is limited to39%dueto small nodule size and difficult access.[8]

One of the most challenging assignments in NSCLC is tracking early disease recurrence, even with very early disease (stage IA), as up to 27%of patients would die as a result of their disease within five years.[9] In a recent cohort, Peled et al. found 4% of early (one year) recurrence by routine bronchoscopy in patients that otherwise had been misdiagnosed due to lack of evidence for disease at the time of bronchoscopy.[6] Therefore, a noninvasive, highly sensitive test, such as detecting characteristic volatile organic compounds (VOCs),[10,11] would be extremely valuable. Such a tool, in a headspace setting, might also be valuable in a laboratory setting, such as for immediate diagnosis of fresh-frozen sections in operating rooms, where a dichotomic diagnosis is crucial for guiding the surgeons with their ongoing surgery.

In this study, we use seven NSCLCs as a pure model for defining the odor print of NSCLCs.[12] For our purposes, the use of cell lines and not tumor tissues could exclude any stromal effect and increase test specificity by detecting the distinctive VOCs that might define NSCLCs. The usage of lung cancer cells has been described recently in the literature. Zhang and coworkers sampled different kinds of lung cancer cells derived from cancerous tissues and other lung-related diseases, but were able to identify and isolate only four VOCs as lung cancer biomarkers.[13] Also, Filipiak and co-workers tested VOCs from lung cancer cell line CALU-1 in vitro, and by using gas chromatography–mass spectrometry (GC–MS) were able to identify 60 compounds that are common both to the specific cell line and to the growth medium. They pointed out which compounds are produced by the cells and which are consumed, since the headspace was tested as a function of time.[14] These GC–MS-based results are promising but the accuracies are not yet high enough to be clinically useful. The benefits of theGC–MS systems include their sensitivity and ability to detect specific VOCs and measure their relative concentrations. The downside is that GC–MS is expensive, requires relatively high expertise to use, and the breath contents need to be captured and preconcentrated before being transported to the devices. Consequently, these systems are not ideal as point-of-care tests.

Herein, we report an array of 18 molecularly modified gold nanoparticles (Au NPs) in combination with a pattern recognition method that can sense and identify patterns of odorant molecule(s), such as VOCs emitted from seven different types of NSCLC, with no need for preconcentration of the lung cancer biomarkers. The molecules surrounding the Au NPs are of the same chemical groups as the VOCs emitted from the NSCLC, and thus show high sensitivity to biomarkers of lung cancer cells. This will help to identify and

discriminate between lung cancer cells and their medium of growth by using principal component analysis (PCA).[15]

2. Results and Discussion

GC–MS analysis identified 350–400 different VOCs that had been either synthesized or catabolized in at least one cell line. The compounds that were chosen for both the NSCLCs and the medium were those with >0.08% of the total amount detected by GC–MS. However, forward stepwise discrimination analysis identified 40 common VOCs that appear in >85% of NSCLCs and of the control medium. The common compounds were mostly nonpolar C_1–C_{13} hydrocarbons. Further forward stepwise discrimination analysis revealed 15 VOCs that appear in all NSCLCs but not in control states (Figure 1). The wide spectrum of compounds detected in our study could be attributed to the effect of solid-phase microextraction (SPME) fibers on the extraction of VOCs. The SPME fiber that we used consisted of polydimethylsiloxane (PDMS), which extracts via absorption with analytes dissolving and diffusing into the bulk of the coating, and PDMS/ divinylbenzene (DVB) and PDMS/ Carboxen (CAR), which “retain” highly volatile solvents and gases.

Based on the GC–MS/SPME data presented in Figure 1, the headspace of cancerous cells included saturated and unsaturated hydrocarbons, benzene derivatives, and oxygen-containing compounds. Most of these compounds have been proven to be connected to cancer through oxidative stress and byproducts of reactive oxygen species (ROS)-inducing processes. It is hypothesized that there is a persistent oxidative stress in cancer cells. For example, it was found that in cancer cells there is a high level of one of the major oxidatively modified DNA base products in vivo, 8-PH-dG, which is known to be formed by radicals. Moreover, it is reasonable to suppose that membrane lipids near the ROS generation site are the most severely damaged.[16] Saturated hydrocarbons that are known to be metabolites of lipid peroxidation[17] and were found in the headspace of the cancer cells support that hypothesis.

Based on these results we designed and used an array of 18 chemiresistors for detecting the headspace of NSCLC and a control medium. In this configuration, each sensor is widely responsive to a variety of odorants.[18] Hence, each analyte yields a distinct signature from the array of broadly cross-reactive sensors.[18] Pattern recognition algorithms can be applied to the multidimensional set of signals, obtained simultaneously from all the sensors in the array, to yield information about the identity, properties, and concentration of the vapor exposed to the sensor array. Figure 2 shows a scheme of the constituent sensors. The functionalities of Au NPs were chosen, based on the GC–MS analysis presented in Figure 1, as having structures similar to the lung-cancer-related biomarkers to maximize the sensitivity to the target analytes. Chemiresistors based on functionalized Au NPs combine the advantages of organic specificity with the robustness and processability of inorganic materials.[19] Au NPs stabilized with thiolated molecules have strong covalent bonds to the sulfur group and, thus, tailor the surface properties of the NPs. Also, sensors of Au NPs that are mostly coated with hydrophobic functionalities are almost insensitive to water and hence are particularly suitable for breath testing, since exhaled breath contains ≈80% relative humidity. A sensor’s high sensitivity to water, as is the case for carbon-nanotube (CNT) sensors, decreases its ability to detect lung cancer.[20]

Prior to exposure to the sample headspace, we examined the response $\Delta R/R_b$ (where R_b, typically ≈1 MΩ, is the baseline resistance of the sensor in the absence of analyte and ΔR is the baseline-corrected steady-state resistance change upon exposure of the sensor to analyte) of each sensor to some representative lung cancer biomarkers (as identified by GC–MS). The biomarker concentrations were P_a/P_o=0.0001–0.05, where P_a and P_o are the partial

pressure and vapor pressure of the analyte at room temperature (≈21 °C), respectively. We found that the sensors' response was rapid upon exposure to the simulated vapor analyte, fully reversible upon switching back to purified dry air, responsive to a wide variety of concentrations, and showed a satisfactory signal-to-noise ratio, typically larger than 10:1. The sensors indicated a detection limit in the order of a few ppb (see representative examples in Table 1), beyond the concentration level of most volatile (cancer) fingerprints that appear in NSCLC.[21]

Figure 3 shows a typical response of three of our sensors to the headspace of NSCLC and the control medium. Again, the response was rapid (limited by the 10-s response time of our vapor-delivery system), completely reversible, and very well reproducible for both NSCLC and the control medium. The sensors showed either a decrease in resistance (ten sensors) or an increase in resistance response (eight sensors). The physical mechanism responsible for the electronic response of NP films to analyte exposure is still subject to controversy. It is well known that the response of chemiresistors made from metal-core NPs and capping monolayers can be either positive (increased resistance) or negative (decreased resistance). These changes could be attributed to one or both of the following mechanisms: 1) swelling, which may increase the resistance due to an increased interparticle tunnel distance; or 2) an increase in the permittivity of the organic matrix surrounding the metal cores may decrease the resistance due to a reduction of the potential barriers between the metal cores, thereby decreasing the tunneling decay constant.[22,23] In this study, we did not monitor the Au NP film morphology[22] or the effect of Au NP size and/or electrode dimensions.

The response to the headspace samples of the 18-sensor array was analyzed by using PCA. This results in the largest variance between sensor values from the first principal component (PC1) and produces decreasing magnitudes of variance from the second (PC2) to the third principal component (PC3), etc. Figure 4 shows PC1, PC2, and PC3 for each sample that accounted for >90% variance. Each data point corresponds to a breath sample. No overlap for the NSCLC and the control patterns is seen, and the clusters were separated with 100% success. Note that clear discrimination was achieved with the sensor array without preconcentration or dehumidification of the cell line sample. This is a marked improvement from our recently demonstrated ten-sensor array based on organically functionalized CNTs, which required adequate pretreatment of a mixture of representative VOCs for clear distinction.[20] Experiments with a wider population of NSCLCs to distinguish thoroughly between the different NSCLCs are under way.

A diagnostic tool that is based on an array of Au NP sensors could include, among other things, inexpensive, noninvasive early detection. Such a tool might narrow the number of the cohort to be investigated, which in turn could lead to an efficient algorithm. In addition, early diagnosis will increase cure rates, especially in lung cancer. Good discrimination ability is important for investigating patients with lung nodules. These patients need invasive assessment as the first step in their evaluation. Therefore, a reliable array of sensors might spare unnecessary thoracic procedures as well as increase the benefits of those actually performed. Another example is the postoperative setting. A reliable breath test will be able to assure complete tumor resection versus recognition of residual tumor that leads to post-operative need for radio/chemotherapy, a capability that might improve overall survival rates in early stage disease.[24]

To put these results in a wider perspective, we examined whether there is a relation between the PCA patterns of the examined (NSCLC and control) cell lines and equivalent states in exhaled breath.[25] Towards this end, exhaled alveolar breath was collected in a controlled way from 40 lung cancer patients (stage 4 and stage 3) and 56 healthy subjects who had not ingested coffee or alcohol for 1 and 12 h, respectively, by using the offline method

recommended by the ATS/ERS[26] (see Reference [27] for details on the collection process of exhaled breath). None of the cancer patients had received chemotherapy and/or other cancer treatment prior to the breath testing. The 40 healthy controls were chosen to match the lung cancer study group in age and lifestyle. In a typical experiment, signals from an array of nine sensors (from the 18 applied for cell lines) were collected for 5 min in a vacuum, followed by 5 min of breath exposure then another 5 min of the vacuum environment.[25] The cycles were typically repeated 3–5 times to test reproducibility.

Plan PC1 versus PC2 of Figure 4 shows the multidimensional $\Delta R/R_b$ data set of cancerous breath and healthy breath.[28] No overlap is seen between the clusters of lung cancer and healthy breath, and the clusters were separated with 100% success (see also Reference [25]). The two-dimensional (2D) patterns of lung cancer breath showed a partial overlapping with the projected (PC1 vs. PC2) patterns of NSCLC. On the other hand, the 2D patterns of healthy breath showed a partial overlapping with the (PC1 vs. PC2) patterns of the control medium. The observed overlapping between the clusters of cell lines and actual breath samples provides clear evidence for the correlation between the biochemical processes appearing in (or in the vicinity of) the cancer cells and the VOCs appearing in exhaled breath, consistent with the recent GC–MS results of Wojciech et al.[21] This finding indicates that an array of Au NP sensors can be used (after further modifications) as a highly sensitive, simple-to-use tool for understanding the biochemical background of endogenous compounds appearing in exhaled breath, both for healthy persons and those suffering from certain diseases such as lung cancer. In this context, the ability to distinguish between different individual biomarkers (see also References [20,29]), as well as between different mixtures (or patterns) of biomarkers, with no need for preconcentration techniques might allow more precise and more robust data than those obtained from GC–MS in combination with preconcentration techniques. This argument is supported by the fact that the latter technique cannot account for all the VOCs present in the headspace or exhaled breath samples, because a preconcentration technique can be thought of as a solid-phase method that extracts only part of the analytes present in the examined phase and afterwards desorbs only part of the extracted analytes.

3. Conclusions

We have identified 40 common VOCs that appear in >85% NSCLCs and in the control medium and 15 VOCs that appear only in NSCLC, but not in the control medium. Based on this knowledge, we fabricated an array of highly sensitive, simple-to-use, and inexpensive cross-reactive sensors and exposed them to NSCLC and the control medium. Analysis of the responses from the array of sensors using PCA showed 100% separation between the clusters of NSCLC and the control medium, without using any preconcentration technique. Success in this endeavor would ultimately provide a launching pad for initiatives for immediate diagnosis of fresh (frozen) tissues of lung cancer in operating rooms, where a dichotomic diagnosis is crucial for guiding surgeons during surgery. The same array may also aid in understanding the biochemical pathway of VOCs from cancer cells to the exhaled breath, without any exclusion, in contrast to traditional methods such as GC–MS in combination with preconcentration techniques, which account for only part of the VOCs in the headspace of cell lines or samples of exhaled breath. From the clinical perspective, a noninvasive, highly sensitive bedside tool has many uses in early detection, therapy evaluation, screening, and therapy direction. Moreover, such a tool in the tissue headspace setting might support immediate decisions taken by surgeons operating on lung cancer patients. The combination with GC–MS would contribute to understanding whether the source of the VOCs is the tumor cells, their microenvironment, or results from the host response to the tumor. However, such understanding has yet to be fully investigated.

4. Experimental Section

Collection of headspace emitted from the cells

Seven NSCLCs of adenocarcinoma were grown in a 100-mm cell-culture dish to 95% confluency (7×10^6 cells) using a medium under standard conditions (RPMI 1640 medium +10% fetal bovine serum; 5% CO_2 environment). A medium with the same incubation time and conditions but without cells served as a control in duplicate. The cell lines were Calu3, H1650, H4006, H1435, H820, H1975, and A549.

Analysis of headspace by GC–MS

Collection of headspace VOCs was carried out with the Ultra II SKC system with Chromosorb 106 as sorbent. All seven cell lines were analyzed by GC–MS (Figure 2). Collected headspace from the NSCLCs and from the control medium (also using the Ultra II system) was transferred to a thermal desorption device made of stainless steel. The sorbents were heated to 270 °C and at the same time were exposed to a SPME fiber of DVB/CAR/PDMS (purchased from Sigma–Aldrich) for preconcentration. The extracted fiber in the manual SPME holder was inserted into the injector of the GC column, which was set to 270°C in the splitless mode. The oven temperature profile was 40 °C for 4 min, 5 °C min^{-1} to 140 °C, held for 4 min, 5 °C min^{-1} to 250 °C, held for 4 min. An H5-5MS capillary column (5% phenyl methyl siloxane; 30 m in length, 0.25 mm internal diameter, 0.25 μm in thickness) was used. The column pressure was set to 8.22 psi, and the initial flow was 0.8 mL min^{-1}. Eventually the molecular structures of the VOCs were determined via the Standard Modular Set.

Synthesis of functionalized Au NPs

Monolayer-capped 5-nm Au NPs were synthesized by the two-phase method[30,31] with some modifications.[31,32] Dodecanethiol, decanethiol, 1-butanethiol, 2-ethylhexanethiol, hexanethiol, *tert*-dodecanethiol, 4-methoxytoluenethiol, octadecanethiol, 3-methyl-1-butanethiol, dibutyl disulfide, 3-mercaptopropionate, 2-mercaptobenzyl alcohol, octadecylamine, 2-mercaptobenzoxazole, and 11-mercapto- 1-undecanol were used as organic capping layers. To synthesize the above-mentioned Au NPs, $AuCl_4^-$ was first transferred from an aqueous $HAuCl_4 \cdot xH_2O$ solution (25 mL, 31.5mM) to a toluene solution by the phase-transfer reagent tetraoctylammonium bromide (TOAB; 80 mL, 34.3mM). After the organic phase was isolated, excess thiol was added to the solution. The molar ratio of thiol to $HAuCl_4 \cdot xH_2O$ was varied between 1:1 and 10:1 depending on the kind of thiol, to prepare a monodispersed solution of Au NPs with an average size of 5 nm. For example, the molar ratios of Au to thiol were 10:1 and 1:1 for dodecanethiol- and butanethiol-capped Au NPs, respectively. After vigorous stirring of the solution for 10 min, an aqueous solution of reducing agent $NaBH_4$ was added in large excess (25 mL, 0.4 M, ice-cooled). The reaction occurred on stirring at room temperature for at least 3 h, which produced a dark brown solution of the thiol-capped Au NPs. The resulting solution was subjected to solvent removal in a rotary evaporator, followed by multiple washings with about 300 mL of ethanol.[11] For further purification, the solutions were released from excess free molecules by using the Millipore system at 55 psi air pressure. Au NPs capped with 2-mercaptobenzoxazole, 3-mercaptopropionate, 3-methyl-1-butanethiol, and 11-mercapto-1-undecanol were synthesized by the ligand-exchange method from preprepared hexanethiol-capped Au NPs. In a typical reaction, excess of incoming thiol, 2-mercaptobenzoxazole (7 μg), was added to a solution of hexanethiol-capped Au NPs in toluene (3 mg mL^{-1}, 5 mL). The solution was stirred constantly for a few days to allow full ligand conversion. The resulting solution was subjected to solvent removal in a rotary evaporator. The NPs were purified from free thiol ligands by repeated extractions.

Design of an array of sensors

An array of sensors was designed by combining 18 different chemiresistors of Au NPs. Ten pairs of circular interdigitated Au electrodes were deposited by electron-beam evaporation on a piece of device-quality silicon wafer capped with 300 nm thermal oxide. Figure 2 shows a schematic illustration of the device. The outer diameter of the circular electrode area was 3000 μm; the gap between two adjacent electrodes and the width of each electrode were both 20 μm. The functionalized Au NPs were dispersed in a suitable solvent by sonication and drop-cast onto the electrodes. While still coated with solution, the substrate was blown dry with N_2. This process was repeated several times to yield the desired resistance of about 1 MΩ. The device was dried at ambient temperature for 2 h and then baked overnight at 50 °C in a vacuum oven.

The headspace of the NSCLC samples was analyzed using the sensor array described above. The sensors were mounted into a custom polytetrafluoroethylene (PTFE) circuit board inside a stainless-steel test chamber with a volume of less than 100 cm^3. The sampling system delivered pulses of breath and ambient air in sequence to the sensors. Alternatively, the chamber could be evacuated. Each sensor of the array underwent a reversible change in electrical resistance when exposed to a vapor or analyte. The responses were unique because of the chemical diversity of the sensor materials. An Agilent multifunction switch 34980 controlled by USB was used to select the active sensor and measure the corresponding resistance at a given time. The entire system was computer controlled. Three analyses, at minimum, were performed on the headspace of each NSCLC sample.

Response measurements from an array of Au NP sensors

All seven NSCLCs were analyzed by an array of sensors using Chromosorb 106 as sorbent material. Collected headspace from the NSCLCs and from the control medium was transferred to a thermal desorption device made of stainless steel. After 30 min of heating the sorbent at 270 °C, the headspace was exposed to the sensor array. Five minutes of vacuum were followed by 5 min of sample exposure; this procedure was repeated three times to obtain three cycles for each sample. Using PCA,[15] data collected from the array of sensors (meaning the change in resistivity in all 18 sensors) was translated into a unique pattern classifying the cancerous cells and the control medium in a three-dimensional plot.

Acknowledgments

This research was funded by a Marie Curie Excellence Grant of the European Commission's FP6 program, the Alfred Mann Institute, the Technion's Russell Berrie Nanotechnology Institute, the SPORE (F.R.H, N.P.), and the IASLC (N.P.). We thank Dr. Gang Peng, Irena Dvorkind, and Meggie Hakim (Technion-IIT) for assistance and fruitful discussions and Dr. Yoshida Koichi for his assistance in the cell culture experiments (UCCC). H.H. holds the Horev Chair for Leaders in Science and Technology.

References

1. Boyle P, Ferlay J. Ann. Oncol. 2005; 16:481. [PubMed: 15718248]
2. Jemal A, Siegel R, Ward E, Hao Y, Xu J, Murray T, Thun MJ. CA Cancer J. Clin. 2008; 58:71. [PubMed: 18287387]
3. Cutler DM. J. Econ. Perspect. 2008; 22:3. [PubMed: 19768842]
4. Garg K, Keith RL, Byers T, Kelly K, Kerzner AL, Lynch DA, Miller YE. Radiology. 2002; 225:506. [PubMed: 12409588]
5. Bach PB, Jett JR, Pastorino U, Tockman MS, Swensen SJ, Begg CB. JAMA. 2007; 297:953. [PubMed: 17341709]
6. Peled N, Flex D, Raviv Y, Fox BD, Shitrit D, Refaeli Y, Saute M, Amital A, Kramer MR. Lung Cancer. 2009 in press.

7. Kirschner PA. Chest Surg. Clin. N. Am. 1996; 6:1. [PubMed: 8646496]
8. Holty JE, Kuschner WG, Gould MK. Thorax. 2005; 60:949. [PubMed: 15994251]
9. Goldstraw P, Crowley J, Chansky K, Giroux DJ, Groome PA, Rami-Porta R, Postmus PE, Rusch V, Sobin L. J. Thorac. Oncol. 2007; 2:706. [PubMed: 17762336]
10. Amann A, Spanel P, Smith D. Mini Rev. Med. Chem. 2007; 7:115. [PubMed: 17305586]
11. Cao W, Duan Y. Crit. Rev. Anal. Chem. 2007; 37:3.
12. Voskoglou-Nomikos T, Pater JL, Seymour L. Clin. Cancer Res. 2003; 9:4227. [PubMed: 14519650]
13. Chen X, Xu F, Wang Y, Pan Y, Lu D, Wang P, Ying K, Chen E, Zhang W. Cancer. 2007; 110:835. [PubMed: 17599760]
14. Filipiak W, Sponring A, Mikoviny T, Ager C, Schubert J, Miekisch W, Amann A, Troppmair J. Cancer Cell Int. 2008; 8:17. [PubMed: 19025629]
15. PCA is a statistical method to effectively reduce our multidimensional data space to its main components and allow convenient visualization of the differentiation ability of the sensor array. PCA determines the linear combinations of the sensor values so that the maximum variance between all data points can be obtained in mutually orthogonal dimensions.
16. Toyokuni S, Okamoto K, Yodoi J, Hiai H. FEBS Lett. 1995; 358:1. [PubMed: 7821417]
17. Kneepkens CMF, Lepage G, Roy CC. Free Radic. Biol. Med. 1994; 17:127. [PubMed: 7959173]
18. Roeck F, Barsan N, Weimar U. Chem. Rev. 2008; 108:705. [PubMed: 18205411]
19. Haick H. J. Phys. D. 2007; 40:7173.
20. Peng G, Trock E, Haick H. Nano Lett. 2008; 8:3631. [PubMed: 18839997]
21. Wojciech F, Andreas S, Tomas M, Clemens A, Jochen S, Wolfram M, Anton A, Jakob T. Cancer Cell Internat. 2008; 8:1.
22. Joseph Y, Guse B, Vossmeyer T, Yasuda A. J. Phys. Chem. C. 2008; 112:12507.
23. Ibañez FJ, Zamborini FP. ACS Nano. 2008; 2:1543. [PubMed: 19206357]
24. Alberts WM. Chest. 2007; 132:1S. [PubMed: 17873156]
25. Peng G, Tisch U, Adams O, Hakim M, Shehada N, Broza YY, Billan S, Abdah-Bortnyak R, Kuten A, Haick H. Nat. Nanotechnol. 2009
26. Silkoff PE, Deykin A, Dweik RA, Laskowski D, Baraldi MD, Lundberg JO, George SC, Marczin N, Metha S. Am. J. Respir. Crit. Care Med. 2005; 171:912. [PubMed: 15817806]
27. The American Thoracic Society/European Respiratory Society (ATS/ERS) method is designed to avoid potential errors due to failure to distinguish between endogenous and exogenous compounds in the breath and to exclude nasal entrainment of gas. The exogenous VOCs are either directly absorbed through the lung via the inhaled breath or indirectly through the blood or skin. The endogenous VOCs are generated by the cellular biochemical processes of the body and, thus, may provide insight into the body's functioning. Based on this method, the people tested cleared the inhaled air of ambient contaminants by repeatedly inhaling to total lung capacity for 5 min through a mouthpiece that contained a filter cartridge on the inspiratory port, thus removing more than 99.99% of the exogenous VOCs from the air during inspiration. Immediately after the lung washout, the subjects exhaled through a separate exhalation port of the mouthpiece against 10–15 cm H_2O pressure to ensure closure of the vellum so that nasal entrainment of gas was excluded. Exhaled breath is a mixture of alveolar air and respiratory dead-space air. In this study, subjects first exhaled the dead-space air into a separate bag and then exhaled the alveolar breath into a 750-mL Tedlar sampling bag (purchased from Eco Medics) made from poly(vinyl fluoride), which is chemically inert with respect to most compounds in the breath. The Tedlar bags were reused and thoroughly cleaned prior to each use with flowing N_2 gas. A minimum of five bags was collected from each person tested.
28. The presentation of the exhaled breath results in 2D space, instead of 3D space, is for the sake of consistency with the results presented in Reference [25].
29. Peng G, Tisch U, Haick H. Nano Lett. 2009; 9:1362. [PubMed: 19320442]
30. Brust M, Walker M, Bethell D, Schiffrin DJ, Whyman R. J. Chem. Soc. Chem. Commun. 1994:801.
31. Brust M, Fink J, Bethell D, Schiffrin DJ, Kiely CJ. J. Chem. Soc. Chem. Commun. 1995:1655.

32. Brust M, Kiely CJ. Colloids Surf. A. 2002; 202:175.
33. Kurdak C, Kim J, Kuo A, Lucido JJ, Farina LA, Bai X, Rowe MP, Matzger A. Appl. Phys. Lett. 2005; 86 073506/1.

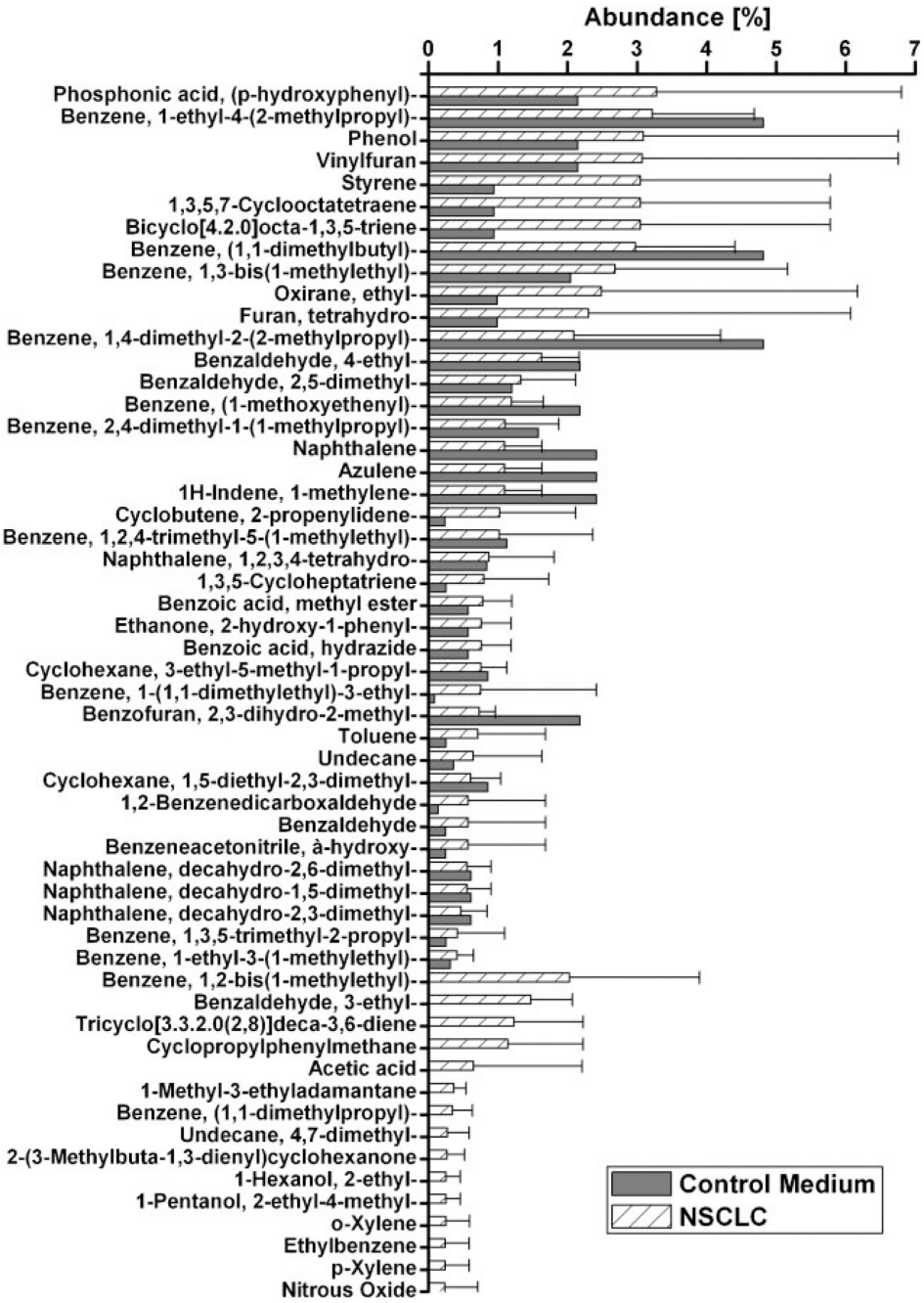

Figure 1.

Average abundance ratio of the 55 volatile biomarkers identified with SPME-aided GC–MS. Forty common VOCs were found in the headspace of NSCLCs and the control cell lines, at distinctly different concentration mixtures. VOCs 41–55 were found only in the headspace of NSCLC samples.

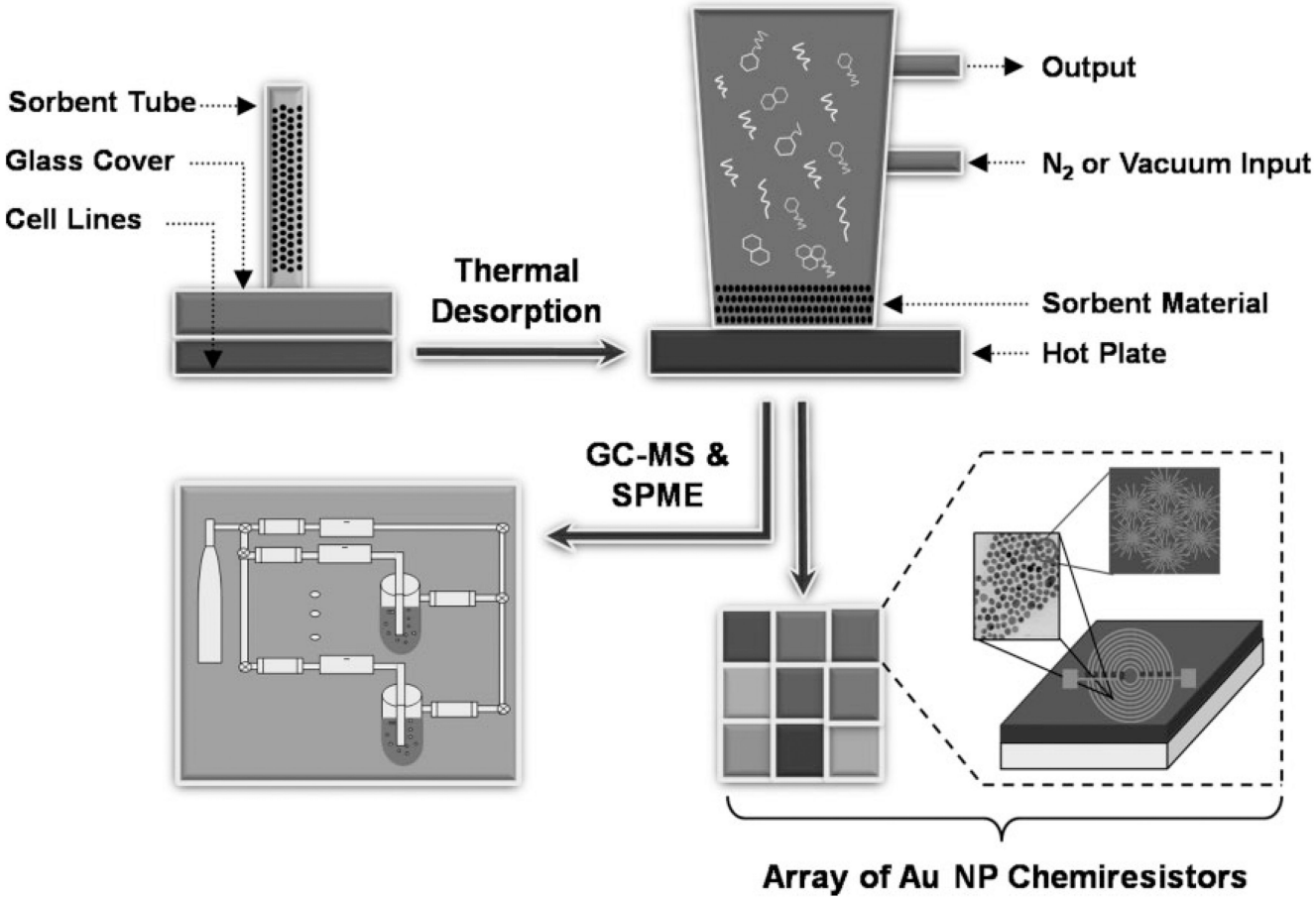

Figure 2.

Schematic representation of the experimental procedures used in this study. The process includes: 1) collecting the headspace of cell lines with sorbent tubes; 2) desorbing the VOCs trapped by the sorbent tube; and 3) analyzing the VOCs by GC–MS and 4) by an array of Au NP sensors in combination with pattern recognition methods. The sensors were formed by successively drop-casting solutions of the molecularly modified NPs onto ten pairs of preprepared Ti/Au interdigitated electrodes. The left-hand inset in the schematic of the sensors shows a transmission electron microscopy (TEM) image of the NPs. The length of the TEM image is 120 nm. The right-hand inset shows films based on molecularly modified Au NPs. In these films, the metallic particles provide the electrical conductivity and the organic film component provides sites for the sorption of analyte (guest) molecules. In addition to their role as an adsorptive phase, the presence of well-defined organic spacers (i.e., capping molecules)allows control over the interparticle distance, and thereby enables nearly uniform interparticle distances to be obtained in the composite films. This allows controlled signal and noise levels to be achieved.[33]

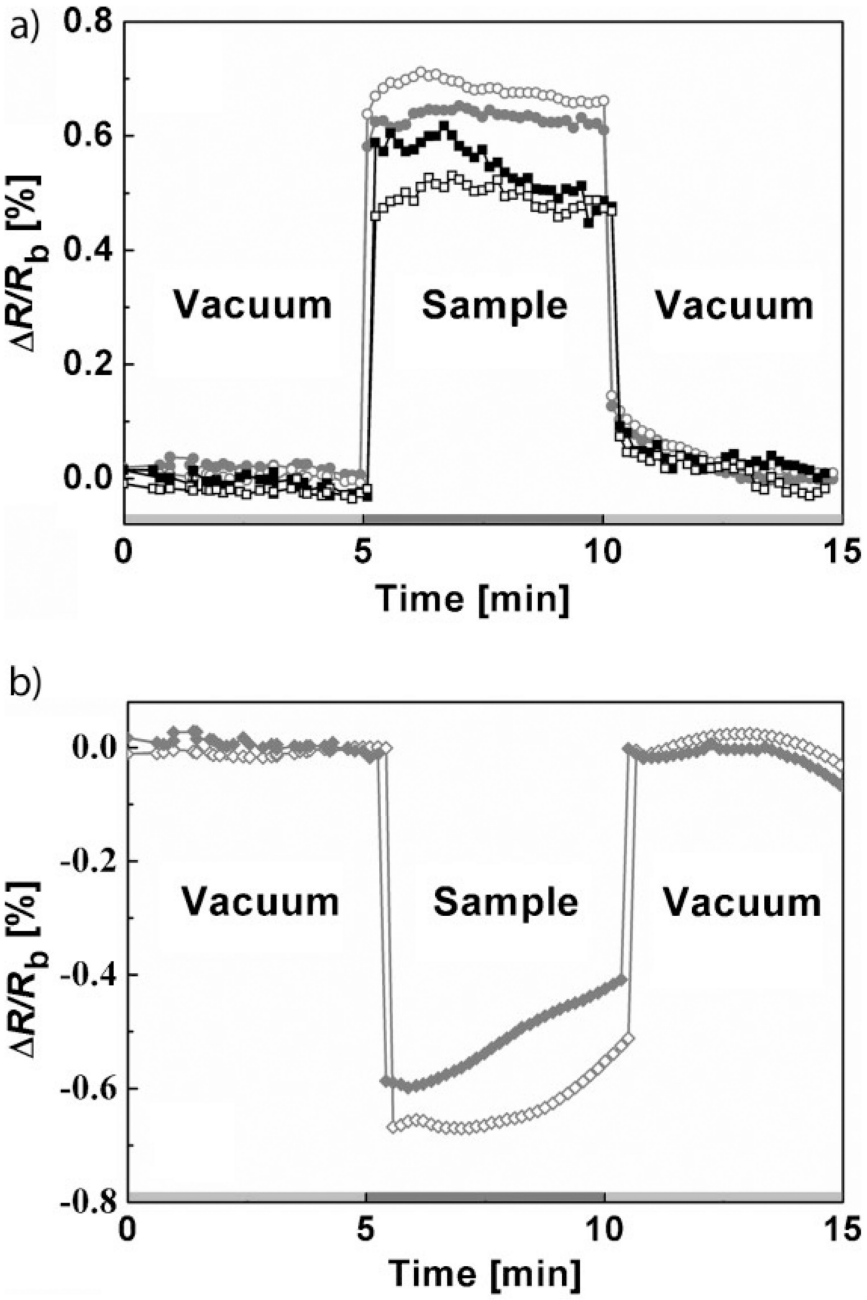

Figure 3.

Typical responses, $\Delta R/R_b$, of a) 2-mercaptobenzoxazole (circles) and 2-mercaptobenzoxazole with 1% carbon black (squares) upon exposure to the headspace of NSCLC (filled symbols) and to control medium (empty symbols), as representative examples of sensors having positive responses, and of b) decanethiol (rhombuses) upon exposure to the headspace of NSCLC (filled symbols) and control medium (empty symbols), as representative examples of sensors having negative responses. The gray lines of the *x* axis indicate that the sensors are under vacuum. Sensors that exhibit higher responses to NSCLC, as compared to control cell lines, indicate that the detected patterns of VOCs are those generated by the cancer cells.[21] Sensors that exhibit higher responses to control cell lines,

as compared to control NSCLC, indicate that the detected patterns of VOCs are those consumed by the cancer cells.[21] The chemical nature and concentration of the generated and consumed VOCs can be seen in the GC–MS results presented in Figure 1.

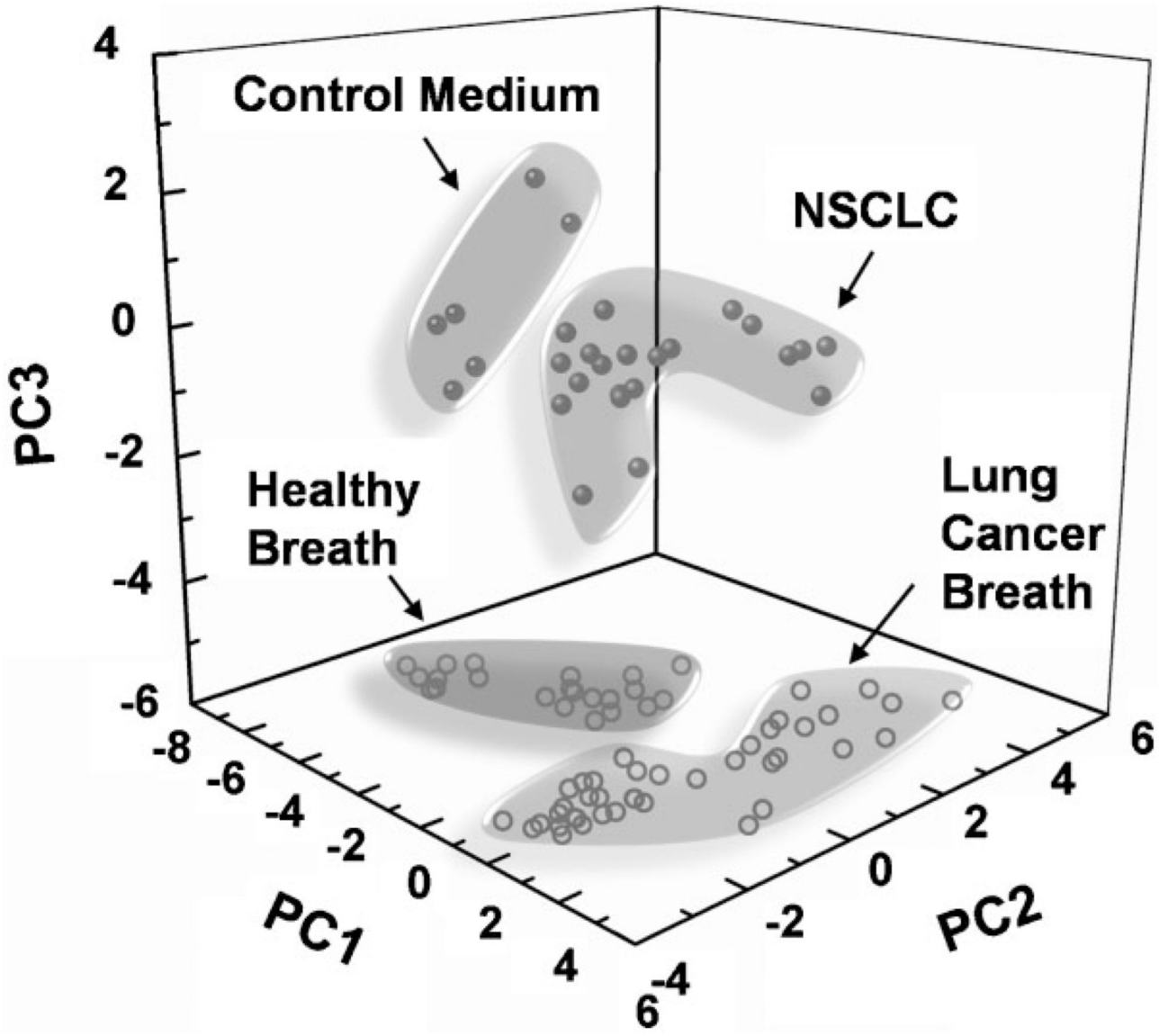

Figure 4.

PCA of the multidimensional $\Delta R/R_b$ data set of NSCLC and control medium. The results yield well-defined clusters for both states, thus allowing fast and reliable examination of lung cancer diagnosis. For the sake of comparison, the PCA results of the multidimensional $\Delta R/R_b$ data set collected (using nine of the sensors applied in this study) from the exhaled breath of patients with primary stage 3 and stage 4 lung cancer and from the exhaled breath of healthy people are presented on the PC1 versus PC2 projection layer. PCA is a statistical method to effectively reduce the multidimensional data space to its main components, to allow convenient visualization of the differentiation ability of the sensor array. PCA determines the linear combinations of the sensor values so that the maximum variance between all data points can be obtained in mutually orthogonal dimensions.

Table 1

Typical resistance response, $\Delta R/R_b$, of a sensor based on Au NPs functionalized with *tert*-dodecanethiol, 2-ethylhexanethiol, and decanethiol upon exposure to vapors of trimethylbenzene at different concentrations. The sensors were responsive to a wide range of concentrations ranging from tens of ppb to hundreds of ppm.

	$\Delta R/R_b$ [%]		
Concentration [ppb]	***Tert*-dodecanethiol-capped Au NPs**	**Decanethiol-capped Au NPs**	**2-Ethylhexanethiol-capped Au NPs**
1000±100	25 ± 2	1.2 ± 0.2	8.1 ± 1.5
900 ± 50	4 ± 1	0.32 ± 0.02	1.5 ± 0.2
500 ± 50	2.1 ± 0.5	0.24 ± 0.02	0.7 ± 0.1
300 ± 50	1.7 ± 0.5	0.11 ± 0.02	0.42 ± 0.05
200 ± 20	1.2 ± 0.2	0.09 ± 0.02	0.23 ± 0.05
100 ± 20	0.6 ± 0.1	0.07 ± 0.02	0.14 ± 0.02
50 ± 20	0.3 ± 0.1	0.05 ± 0.02	0.08 ± 0.01
10 ± 5	0.05 ± 0.01	0.02 ± 0.02	0.021 ± 0.01